LAWRENCE
LIVERMORE
NATIONAL
LABORATORY

LLNL-JRNL-645663

# Atmospheric Tides in the Latest Generation of Climate Models

C. Covey, A. Dai, R. S. Lindzen, D. Marsh

November 4, 2013

Journal of the Atmospheric Sciences

## Disclaimer

# Atmospheric Tides in the Latest Generation of Climate Models

Curt Covey

*Program for Climate Model Diagnosis and Intercomparison, Lawrence Livermore National Laboratory, Livermore, CA*

Aiguo Dai

*University at Albany, State University of New York, Albany, NY*

Richard S. Lindzen

*Massachusetts Institute of Technology, Cambridge, MA*

Daniel R. Marsh

*National Center for Atmospheric Research, Boulder, CO*

For submission to *The Journal of the Atmospheric Sciences*

(expedited review)

---

*Corresponding author address:* Curt Covey, LLNL Mail Code L-103, 7000 East Avenue, Livermore, CA 94550
E-mail: covey1@llnl.gov

LLNL-JRNL-645663

ABSTRACT

For atmospheric tides driven by solar heating, the database of climate model output used in the most recent assessment report of the Intergovernmental Panel on Climate Change (IPCC) confirms and extends our earlier results based on the previous generation of models. Both the present study and the earlier one examine the surface-pressure signature of the tides, because that is their best-observed feature, but the new database removes a shortcoming of the earlier study in which model simulations were not strictly comparable to observations. The present study confirms an approximate consistency among observations and all model simulations, despite variation of model tops from 31 to 144 km. On its face this result is surprising because atmospheric tides are driven in large part by solar heating of the ozone layer (30 – 70 km altitude). Classical linear tide calculations and occasional numerical experimentation have long suggested that models with low tops achieve their consistency with observations by means of compensating errors, with wave reflection from the model top making up for a lack of ozone forcing. Future work with the new database may confirm this hypothesis by extending our purview to free atmosphere fields. The new generation of models is suitable for such work because many of them include the entire middle atmosphere.

## 1. Introduction: New model output

This paper updates our earlier study of atmospheric tides in climate-oriented general circulation models (Covey et al. 2011, hereafter CDML). The tides interact with many surface and higher-altitude processes that play important roles in atmospheric dynamics and climate. CDML found a surprising consistency of model simulations with each other and with observations. This is surprising because atmospheric tides are driven in large part by solar heating of the ozone layer (Chapman and Lindzen 1970) and many of the models have a limited vertical domain that does not include the full range of ozone heating (30 – 70 km altitude, Chapman and Lindzen 1970). CDML's results were consistent with previous work dating back to Lindzen et al. (1968) suggesting that when a model's upper boundary is placed at low altitude, a cancellation of errors can occur—reducing the forcing of tides by ozone heating, but also introducing spurious waves by reflection at the boundary.

A significant shortcoming of CDML arose from a limitation of its climate model output database (CMIP3 / IPCC AR4; see Meehl et al. 2007). Both CDML and the present study examine the surface-pressure signature of the tides because that is their best-observed feature. Analogous to oceanic tides, atmospheric tides appear as oscillations of vertically integrated fluid mass, i.e. of surface pressure. The CMIP3 database, however, included sea level pressure but not actual surface pressure in its high-time-frequency fields. Comparison of observed surface pressure with model-generated sea level pressure was problematic over elevated terrain, where the concept of equivalent sea level pressure is ambiguous. Fortunately, a new version of

the database includes surface pressure at 3-hourly frequency (CMIP5 / IPCC AR5; see Taylor et al. 2012). The new database also incorporates the latest generation of climate models, which cover a greater altitude range (Table 1).

Table 1 in this paper is the analog of Table 1 in CDML but with a more careful definition of model top. Models use staggered vertical levels with one set ("layer midpoints" or "full levels") carrying temperature and other thermodynamic fields, and a second set ("layer interfaces" or "half levels") carrying vertical velocity and other flux fields. Vertical coordinates are pressure-based from the middle stratosphere upward. As shown in the table, several of the models put their topmost half level at zero pressure. Using half levels to define a model's top would imply that these models extend infinitely upward. To avoid this, we use full- rather than half levels to define the vertical extent of models. For the present work we considered 23 CMIP5 models featured in recent studies of stratospheric dynamics (Driscoll et al. 2012, Wilcox et al. 2012, Charlton-Perez et al. 2013, Marsh et al., 2013). Six of these models not providing 3-hourly output (or not providing it in standard form) had to be omitted, leaving 17 models for this study. Ten of our 17 models include all of the stratosphere (topmost full level $\geq$48 km). Five include all of the stratosphere and mesosphere (topmost full level $\geq$76 km). In CMIP3 the corresponding fractions were 5/23 all-stratosphere and 0/23 all-stratosphere + mesosphere (Cordero and Forster 2010). One model (WACCM4) has by far the highest full level in CMIP5, extending well into the thermosphere.

## 2. Comparison with observations

Here we compare CMIP5 model output with the observed surface pressure data employed by CDML (Dai and Wang 1999). These remain the best high-frequency direct observations. Future studies may find it profitable to examine reanalysis of the direct observations via initialization algorithms for numerical weather prediction (NWP, which has produced reasonable tidal oscillations; see e.g. Ray and Ponte 2003). Like reanalysis of other fields, this would involve a tradeoff. NWP models impose known conservation laws for mass, momentum and energy, hopefully eliminating unphysical anomalies, but one can ask how much of the reanalyzed data comes from real observations versus to a model's "opinion" of what the data ought to be. Near-surface pressure is not expected to suffer much from this problem (see Table 4 in Kalnay et al. 1996) but for the present work we choose the direct observations. This permits direct comparison of the present results with CDML.

For the same reason, we process the model output in exactly the same way as CDML. Observations of December-January-February for 1976-97 are compared with model output for 1 January 2000 – 1 February 2000 inclusive (giving an exact power of 2 time points as input to fast Fourier transforms). CDML's Appendix shows that, unlike the tides' upper atmospheric signature (e.g., Burrage et al. 1995, Wu et al. 2008), surface pressure tide variations exhibit only small inter-annual variability.

115 *a. Tidal amplitude*

116 Figures 1 and 2 show maps of CMIP5 diurnal and semidiurnal tidal
117 amplitudes, using the same color scales as the corresponding CMIP3 maps (CDML
118 Figs. 2 – 3 respectively). For these figures we have selected CMIP5 models with
119 lowest (upper left), second highest (upper right) and highest (lower left) full levels.
120 Only January results are shown to save space; July results are similar, as shown in
121 Table 2.

122 The CMIP5 diurnal harmonic amplitude maps (Fig. 1) differ noticeably from
123 their CMIP3 analogs for the models with lowest (INMCM4) and second highest
124 (MIROC-ESM) tops. For CMIP5 these two maps exhibit less excessively large
125 amplitudes than the analogous maps for CMIP3, e.g. the maximum value in INMCM3
126 (> 360 Pa) has been reduced to a more reasonable 249 Pa in INMCM4 (vs. an
127 observed maximum value of 141 hPa). The difference between CMIP5 and CMIP3
128 becomes more striking when one recalls that CDML's figures excluded high
129 elevation terrain, in which the tidal amplitude was even more egregious. There
130 seems little doubt that the improvement in CMIP5 data is mainly due to the use of
131 actual surface pressure. INMCM4 is a revised version of INMCM3, and we find no
132 reason to suppose the revisions significantly altered this model's tide simulations;
133 apparently the better result shown here is simply due to CMIP5 saving more
134 appropriate output data. WACCM4 differs from WACCM3 (used in CDML) primarily
135 by coupling to a deep-ocean model, as opposed to prescribing observed sea surface
136 temperatures (Marsh et al., 2013). CDML showed this choice makes very little
137 difference in tidal simulations, and here the CMIP5 WACCM map differs little from

its previous version. The main difference is the increase in maximum values from 149 Pa in WACCM3 to 178 Pa in WACCM4.

Other than the differences noted above, CMIP5 diurnal harmonic maps are similar to their CMIP3 analogs. In particular, the models with the lowest and second highest tops (upper panels) produce amplitudes that are very much alike despite nearly a factor of 3 difference in their vertical coverage. INMCM4 with its topmost full level at 31 km excludes most ozone heating, while MIROC-ESM with its topmost full level at 86 km includes all of it, yet both overestimate diurnal amplitude by the same amounts over the same land areas. WACCM in contrast obtains much better agreement with observations (lower panels). Another feature shared by the CMIP3 and CMIP5 maps is a larger than observed spatial variability at middle and high latitudes. The smaller variability in the observed map, however, may be an artifact of smoothing procedures used by Dai and Wang (1999).

For the semidiurnal harmonic, CMIP5 amplitude maps (Fig. 2) do not differ as much from their CMIP3 analogs as they do for the diurnal harmonic. The map for INMCM4, however, does reduce some excessive amplitude values that appeared over tropical land areas, bringing the maximum value—over 180 Pa in INMCM3—into better agreement with observation. Again this improvement is likely due to the use of actual surface pressure in the CMIP5 database. The result shown here for WACCM4 is very close to that shown by CDML for WACCM3, with identical-looking patterns, and maximum and mean values differing by less than 2%. As with the diurnal harmonic, MIROC-ESM obtains uniformly higher amplitudes than WACCM4.

Table 2 (analogous to CDML's Table 3) provides a more quantitative point of view of the foregoing points. It shows three measures of model – observation agreement from maps like those in Figs. 1 – 2: the global mean of model / observed amplitude ratio $R$, the model-observed spatial correlation $\rho$, and the model-observed root mean square difference $\Delta$. These three measures are independent. A fourth measure, the model / observed ratio of variances, is dependent on $\rho$ and $\Delta$; it is often shown in a two-dimensional Taylor (2001) diagram that omits $R$.

Comparing the two versions of WACCM, very little difference appears in any of the three measures. Comparing the two different versions of INMCM, one must be cautious because the output available from INMCM3 was sea level pressure rather than surface pressure. This tended to inflate $R$ at low latitudes, making up for an underestimate of amplitude at higher latitudes (see Figs. 1 – 3 in CDMS). Thus INMCM3's "better" values of global mean $R$, compared with INMCM4's values, may be spurious. The other numbers are about the same in the two versions of INMCM except for $\Delta$, which is substantially lowered in INMCM4's diurnal harmonics. The numbers for MIROC-ESM are fairly close to the numbers for INMCM4 except for $R$. Global mean $R$ is closer to unity for MIROC-ESM, but inspection of Figs. 1 – 2 shows that this model (and WACCM4) achieves this result by averaging low latitude overestimates with high latitude underestimates.

In short, although the models INMCM, MIROC-ESM and WACCM span the range of altitude coverage in CMIP5, with topmost full levels at 31, 86 and 144 km respectively, they exhibit relatively small differences in the accuracy of their tidal amplitude simulations.

Fig. 3 (analogous to CDML's Fig. 8a) shows, for January, the equatorial Fourier longitude-transformed amplitudes of all 17 CMIP5 models and observations as a function of zonal wavenumber *s*. This allows isolation of the "migrating" components of the tides that follow the apparent motion of the Sun across the sky, i.e. $s = 1$ for the diurnal harmonic and $s = 2$ for the semidiurnal harmonic. The migrating components dominate both harmonics in models and observations, but all of the models overestimate migrating amplitudes (by up to a factor of 2). These results were also noted by CDML for the CMIP3 models. Also apparent both in Fig. 3 and in the analogous CMIP3 output are secondary peak diurnal amplitudes at $s = -3$ and +5, symmetric about the diurnal migrating component at $s = 1$. The observed peaks are much smaller than the model-simulated peaks. If the peaks were symmetric about $s = 0$, they would combine to form a standing wave; here there is probably enough symmetry for the sum to give localized oscillations. Thus the discrepancy between models and observations relates to the local diurnal cycle of surface pressure, and presumably to the diurnal cycle of temperature and other fields as well. We believe it is worth future investigation.

*b. Tidal phase*

Fig. 4 shows, for January, the zonal mean values of the local time of maximum surface pressure for all 17 CMIP5 models and observations as a function of latitude. July results (not shown) are similar. This is one measure of the phase of the tides. CDML showed a somewhat different measure: the phase of the migrating component obtained by Fourier analysis (see preceding subsection and CDML Fig.

9). While isolating the migrating component provides a connection to classical linear tide theory (Chapman and Lindzen 1970) it does not allow direct comparison with observations (Dai and Wang 1999) since the latter include phase information only for the combination of all zonal wavenumbers. Phase diagrams for the migrating components of CMIP5 tides (not shown here) strongly resemble their CMIP3 analogs and deliver the same basic message as Fig. 4.

The basic message (as in CDML) is that in the tropics, where tidal amplitude is strongest, model-simulated times of maximum are about 0600 LST for the diurnal harmonic and 1000/2200 LST for the semidiurnal harmonic. This agrees approximately with observations, but Fig. 4 allows a more precise comparison. In the tropics, the model-simulated diurnal harmonic's time of maximum is up to 2 hours earlier than observations indicate, and the model-simulated semidiurnal harmonic's time of maximum ranges from about half an hour earlier to half an hour later than observed, depending on the model. Outside the tropics, in both models and observations, the diurnal time of maximum increases steadily with latitude, while the semidiurnal time of maximum decreases. An obvious discrepancy between model-simulated and observed semidiurnal phase occurs in southern (summer) mid-latitudes where the models retain their tropical time of maximum, while observations indicate that the time of maximum shifts to several hours earlier. As with tidal amplitude, there is no obvious correlation between the accuracy of model-simulated phase and a model's vertical domain. For example, the six models producing the most accurate semidiurnal phase near the Equator are INMCM4, CCSM4, HadGEM2-A, MIROC5, GISS-E2-R and WACCM4. These models have topmost

full levels at 31, 38, 39, 40, 64 and 144 km respectively, spanning the full range for the models studied here.

## 3. Conclusions

The approximate consistency of CMIP3 and CMIP5 tide simulations with each other and with observations occurs despite the fact that the lowest-top model (INMCM) extends only into the middle stratosphere, whereas the highest-top model (WACCM) extends well into the thermosphere. As noted in the Introduction, classical linear tide calculations suggest that the lower-top models achieve their consistency with observations by means of compensating errors, with wave reflection from the model top making up for a lack of ozone forcing (Lindzen et al. 1968; see also Zwiers and Hamilton 1986 and Hamilton et al. 2008). The CMIP5 database now provides an "apples-to-apples" comparison with observations in terms of actual surface pressure, further supporting the compensating errors hypothesis. Confirmation of the hypothesis, however, will require direct examination of wave propagation in and above the ozone layer, e.g. classical linear calculations with vertical discretization matching the various CMIP models.

Other future work could go beyond the surface signature of the tides and examine free-atmosphere fields. The CMIP5 database provides temperature, winds and humidity on all model levels at 6-hourly frequency. This should suffice for study of the (dominant) diurnal harmonic in and above the stratosphere. In a broader sense, the extension of CMIP5 models to include the middle atmosphere (Table 1) offers a new domain of climate model inter-comparison.

**Acknowledgements**

We acknowledge the World Climate Research Program's Working Group on Coupled Modeling, which is responsible for CMIP, and we thank the climate modeling groups (listed in Table 1 of this paper) for producing and making available their model output. For CMIP the U.S. Department of Energy's Program for Climate Model Diagnosis and Intercomparison provides coordinating support and led development of software infrastructure in partnership with the Global Organization for Earth System Science Portals. This work was performed under auspices of the Office of Science, US Department of Energy, by Lawrence Livermore National Laboratory under Contract DE-AC52-07NA27344, and in part at the National Center for Atmospheric Research, sponsored by the National Science Foundation.

## References

Burrage, M. D., M. E. Hagan, W. R. Skinner, D. L. Wu, and P. B. Hays, 1995: Long-term variability in the solar diurnal tide observed by HRDI and simulated by the GSWM. *Geophys. Res. Lett.*, **22**(19), 2641–2644, doi:10.1029/95GL02635.

Chapman, S., and R. S. Lindzen, 1970: *Atmospheric Tides*. D. Reidel, 200 pp. + ix.

Charlton-Perez, A. J., and Coauthors, 2013: On the lack of stratospheric dynamical variability in low-top versions of the CMIP5 models, *J. Geophys. Res.*, **118,** 1-12.

Cordero, E. C., and P. M. de Forster, 2006: Stratospheric variability and trends in models used for the IPCC AR4. *Atmos. Chem. Phys.* **6,** 369-5380.

Covey, C., A. Dai, D. Marsh, and R. S. Lindzen, 2011: The surface-pressure signature of atmospheric tides in modern climate models. *J. Atmos. Sci.*, **68,** 495-514.

Dai, A., and J. Wang, 1999: Diurnal and semidiurnal tides in global surface pressure fields. *J. Atmos. Sci.*, **56,** 3874-3890.

Deque, M., C. Dreveton, A. Braun, and D. Cariolle, 1994: The ARPEGE/IFS atmosphere model—A contribution to the French community climate modeling. *Climate Dynamics*, **10,** 249-266.

Driscoll, S. A. Bozzo, L. J. Gray, A. Robock, and G. Stenchikov, 2012: Coupled Model Intercomparison Project 5 (CMIP5) simulations of climate following volcanic eruptions. *J. Geophys. Res.*, **117,** D17105, doi:10.1029/2012JD017607.

Hamilton, K., S. C. Ryan, and W. Ohfuchi, 2008: Orographic effects on the solar semidiurnal surface tide simulated in a very fine resolution general circulation model. *J. Geophys. Res.*, **113,** D17114.

Kalnay, E., and Coauthors, 1996: The NCEP / NCAR 40-year reanalysis project. *Bull. Amer. Meteor. Soc.*, **77,** 437-471.

Lindzen, R.S., E.S. Batten, and J.-W. Kim, 1968: Oscillations in atmospheres with tops. *Mon. Wea. Rev.*, **96,** 133-140.

Marsh, D. R., M. Mills, D. Kinnison, J.-F. Lamarque, N. Calvo, and L. Polvani, 2013: Climate change from 1850 to 2005 simulated in CESM1(WACCM). *J. Clim.,* 26(19), 7372–7391, doi:10.1175/JCLI-D-12-00558.

Meehl, G.A, C. Covey, T. Delworth, M. Latif, B. McAvaney, J.F.B. Mitchell, R.J. Stouffer and K.E. Taylor, 2007: The WCRP CMIP3 multimodel dataset: A new era in climate change research. *Bull. Amer. Meteor. Soc.*, **88,**1383-1394.

Randall, D.A., and Coauthors, 2007: Climate Models and Their Evaluation. In: *Climate Change 2007: The Physical Science Basis*. Contribution of Working Group I to the Fourth Assessment Report of the Intergovernmental Panel on Climate Change, S., Solomon, D. Qin, M. Manning, Z. Chen, M. Marquis, K. B. Averyt, M. Tignor and H.L. Miller, Eds. Cambridge University Press, 589-662.

Ray, R. D., and R. M. Ponte, 2003: Barometric tides from ECMWF operational analyses. *Ann. Geophysicae*, **21,** 1897-1910.

Taylor, K. E., 2001: Summarizing multiple aspects of model performance in a single diagram. *J. Geophys. Res.* **106,** 7183-7192.

Taylor, K. E., R. J. Stouffer, and G. A. Meehl, 2012: An overview of CMIP5 and the experiment design. *Bull. Amer. Meteor. Soc.,* **93,** 485-498.

Voldoire, A., and Coauthors, 2013: The CNRM-CM5.1 global climate model: description and basic evaluation. *Climate Dynamics,* **40,** 2091-2121.

311 Wilcox, L. J., A. J. Charlton-Perez, and L. J. Gray, 2012: Trends in Austral jet position
312 in ensembles of high- and low-top CMIP5 models. *J. Geophys. Res.*, **117**, D13115,
313 doi:10.1029/2012JD017597.
314 Wu, Q., D. A. Ortland, T. L. Killeen, R. G. Roble, M. E. Hagan, H.-L. Liu, S. C. Solomon, J.
315 Xu, W. R. Skinner, and R. J. Niciejewski, 2008: Global distribution and
316 interannual variations of mesospheric and lower thermospheric neutral wind
317 diurnal tide: 1. Migrating tide, *J. Geophys. Res.*, 113, A05308,
318 doi:10.1029/2007JA012542.
319 Zwiers, F. and K. Hamilton, 1986: Simulation of solar tides in the Canadian Climate
320 Center General Circulation Model. *J. Geophys. Res.* **91,** 11877-11896.
321
322
323

TABLE 1. CMIP5 models for atmospheric tide studies.

| | Name of model | Top full-/half-level | Layers[a] |
|---|---|---|---|
| 1 | **BCC-CSM1.1** | 3.6/2.2 hPa ( 38/ 42 km) | 26 ( 2) |
| 2 | **CanAM4** | 1.0/0.5 hPa ( 48/ 54 km) | 35 ( 3) |
| 3 | **CCSM4** | 3.6/2.2 hPa ( 38/ 42 km) | 26 ( 2) |
| 4 | **CNRM-CM5** [b] | 10.0/ 0 hPa ( 31/ ∞ km) | 31 ( 1) |
| 5 | **GFDL-CM3** | 0.02/0.01 hPa ( 76/ 80 km) | 48(13) |
| 6 | **GFDL-ESM2M** | 3.7/1.0 hPa ( 38/ 48 km) | 24 ( 1) |
| 7 | **GISS-E2-R** | 0.14 /0.10 hPa ( 64/ 66 km) | 40 ( 8) |
| 8 | **HadGEM2-A** | 3.2/2.1 hPa ( 39/ 42 km) | 38 ( 2) |
| 9 | **INMCM4** | 10.0/ 0 hPa ( 31/ ∞ km) | 21 ( 1) |
| 10 | **IPSL-CM5A-LR** | 0.04/0 hPa ( 72/ ∞ km) | 39 ( 9) |
| 11 | **IPSL-CM5A-MR** | 0.04/0 hPa ( 72/ ∞ km) | 39 ( 9) |
| 12 | **MIROC5** | 2.9/ 0 hPa ( 40/ ∞ km) | 40 ( 2) |
| 13 | **MIROC-ESM** | 0.004/0 hPa ( 86/ ∞ km) | 80(33) |
| 14 | **MIROC-ESM-CHEM** | 0.004/0 hPa ( 86/ ∞ km) | 80(33) |
| 15 | **MRI-CGCM3** | 0.01/0 hPa ( 80/ ∞ km) | 48(11) |
| 16 | **NorESM1-M** | 3.6/2.2 hPa ( 38/42 km) | 26 ( 2) |
| 17 | **WACCM4** | $6/5\times10^{-6}$ hPa (144/148 km) | 66(18) |

[a] Total number of vertical layers, and (in parentheses) number of layers at altitudes with large solar UV absorption by ozone (30 km < z < 70 km).

[b] Previous version (CNRM-CM3) had the *highest* full-level of all CMIP3 models: 0.05 hPa (76 km; see Deque et al. 1994 and Randall et al. 2007). For CMIP5 "it has been decided to reduce the number of levels because of constraints on computing resources . . ." (Voldoire et al. 2013).

TABLE 2. Comparison of observed surface pressure tidal amplitude with model-simulated tidal amplitude from selected CMIP5 / IPCC AR5 models, WACCM3 (surface pressure output, unmasked) and from INMCM3, a CMIP3 / IPCC AR4 model (sea level pressure output, masked). *

| Model | Harmonic | Month | Global mean model/obs ratio | Model – obs correlation | Model – obs rms difference [Pa] |
|---|---|---|---|---|---|
| WACCM3 | Diurnal | January | 0.681 | 0.673 | 25.9 |
| WACCM4 | | | 0.658 | 0.692 | 26.7 |
| WACCM3 | Diurnal | July | 0.733 | 0.620 | 25.1 |
| WACCM4 | | | 0.745 | 0.549 | 27.8 |
| WACCM3 | Semidiurnal | January | 0.962 | 0.943 | 20.1 |
| WACCM4 | | | 0.950 | 0.942 | 21.1 |
| WACCM3 | Semidiurnal | July | 0.946 | 0.910 | 19.7 |
| WACCM4 | | | 0.965 | 0.907 | 20.2 |
| INMCM3 | Diurnal | January | 0.808 | 0.703 | 39.6 |
| INMCM4 | | | 0.767 | 0.652 | 30.1 |
| INMCM3 | Diurnal | July | 0.944 | 0.739 | 39.9 |
| INMCM4 | | | 0.786 | 0.622 | 28.1 |
| INMCM3 | Semidiurnal | January | 0.920 | 0.912 | 20.6 |
| INMCM4 | | | 0.726 | 0.937 | 19.2 |
| INMCM3 | Semidiurnal | July | 0.914 | 0.885 | 19.4 |
| INMCM4 | | | 0.708 | 0.904 | 20.3 |
| MIROC-ESM | Diurnal | January | 0.839 | 0.677 | 28.1 |
| MIROC-ESM | Diurnal | July | 0.832 | 0.585 | 28.9 |
| MIROC-ESM | Semidiurnal | January | 1.065 | 0.941 | 27.6 |
| MIROC-ESM | Semidiurnal | July | 1.062 | 0.905 | 27.1 |

* "Unmasked" means that comparison is made over the entire surface area of Earth. "Masked" means that land areas with elevation > 1 km are excluded from the comparison. INMCM3, WACCM3 values are repeated from Table 3 in Covey et al. (2011).

**Figure Captions**

FIG. 1. Amplitudes (Pa) of diurnal harmonics of January surface pressure from (top, bottom right) three CMIP5 / IPCC-AR5 climate models and (bottom right) observations (Dai and Wang 1999).

FIG. 2. As in Fig. 1, but for the semidiurnal harmonics; note different color scale

FIG. 3. Fourier longitude amplitude at the equator vs. zonal wavenumber for (top) diurnal and (bottom) semidiurnal harmonics of (thin colored lines) all CMIP5 / IPCC AR5 climate models in this study and (thick black line) observations for January. Closeups show details of peaks in the vicinity of migrating Fourier-component wavenumbers (red vertical lines).

FIG. 4. January tidal phase vs. latitude for (thick black line) observations and for all CMIP5 / IPCC AR5 climate models in this study. See Fig. 3 for line legend distinguishing the different models.

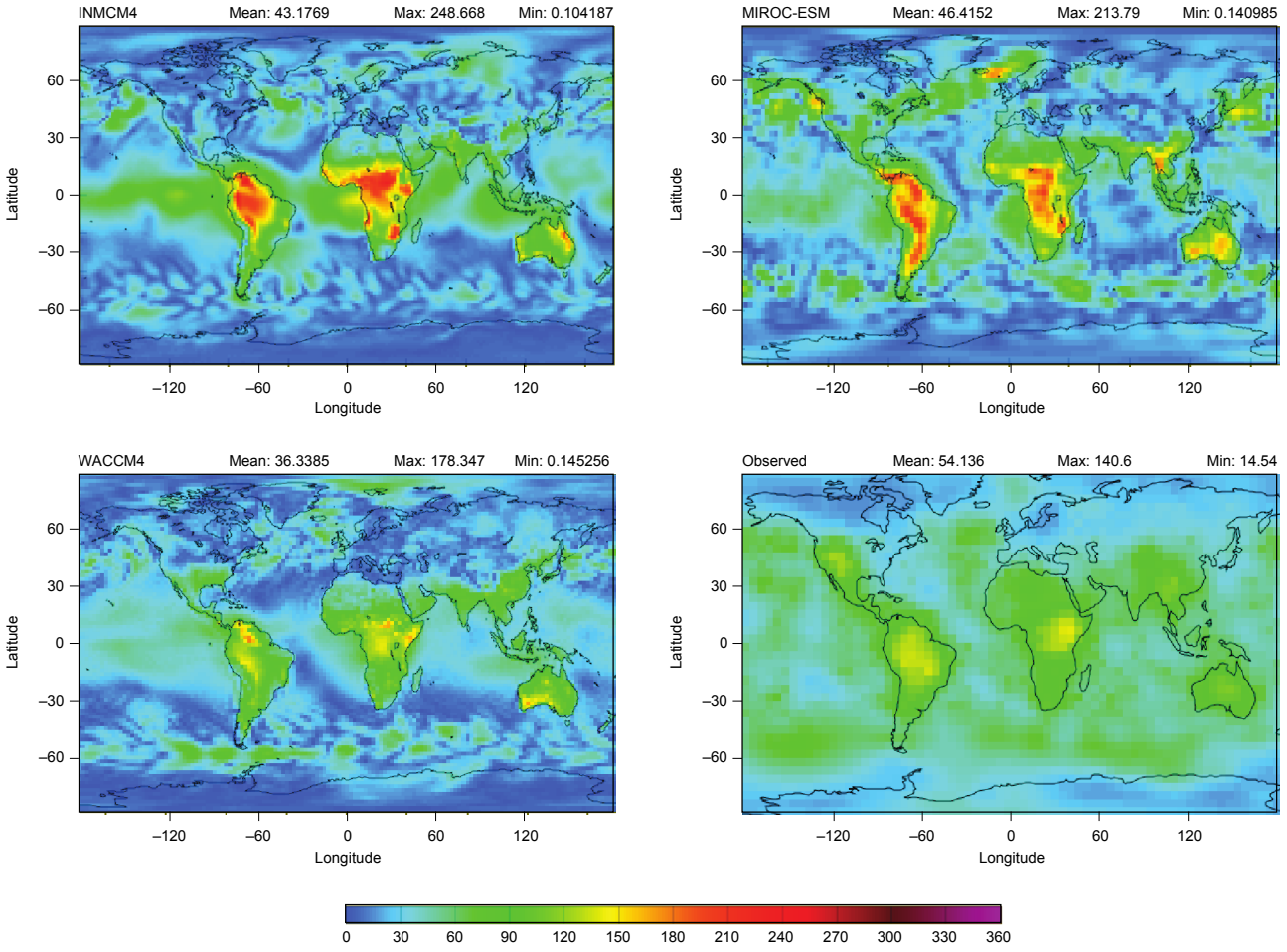


FIG. 1. Amplitudes (Pa) of diurnal harmonics of January surface pressure from (top, bottom right) three CMIP5 / IPCC-AR5 climate models and (bottom right) observations (Dai and Wang 1999).

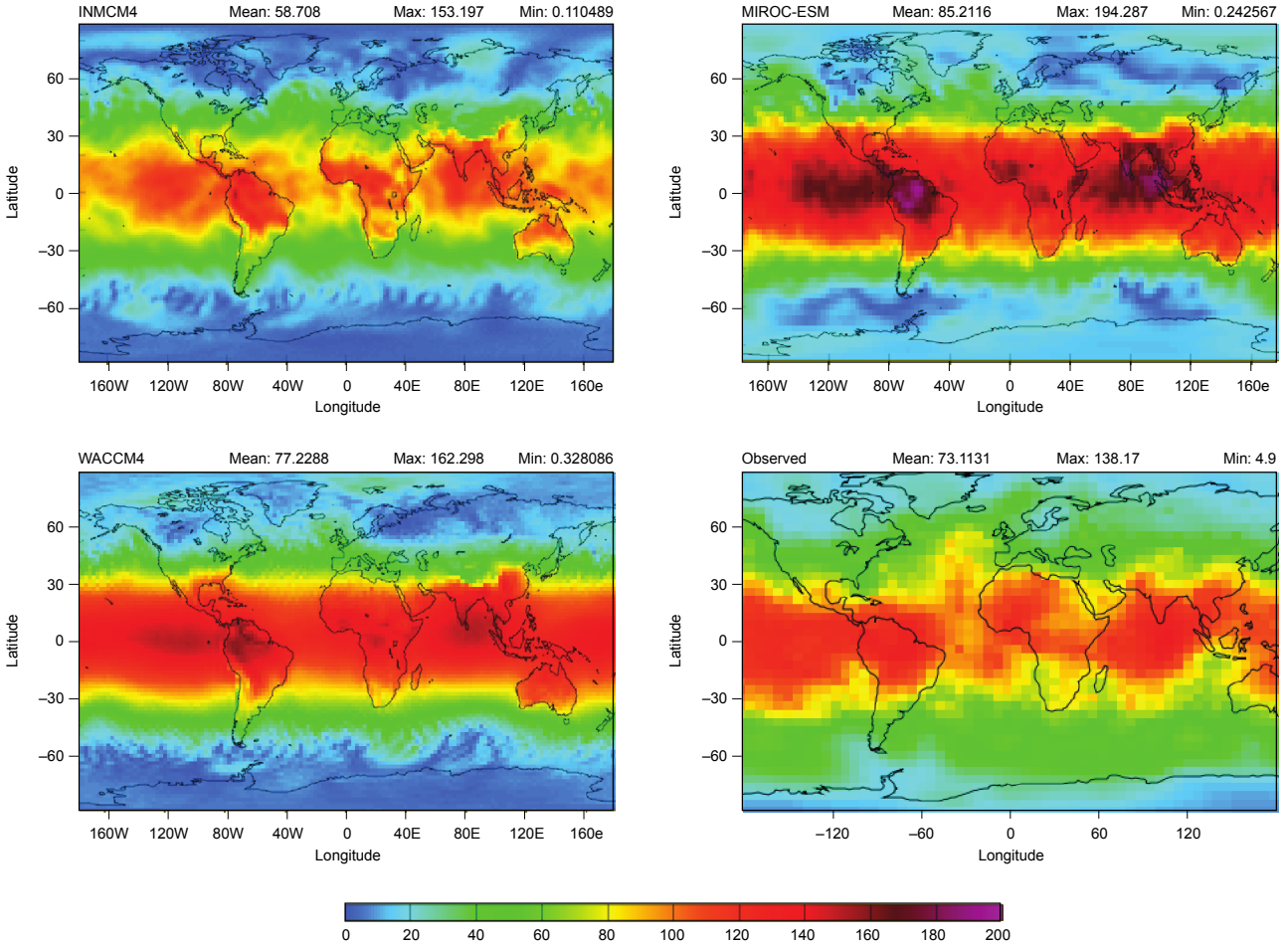


FIG. 2. As in Fig. 1, but for the semidiurnal harmonics; note different color scale.

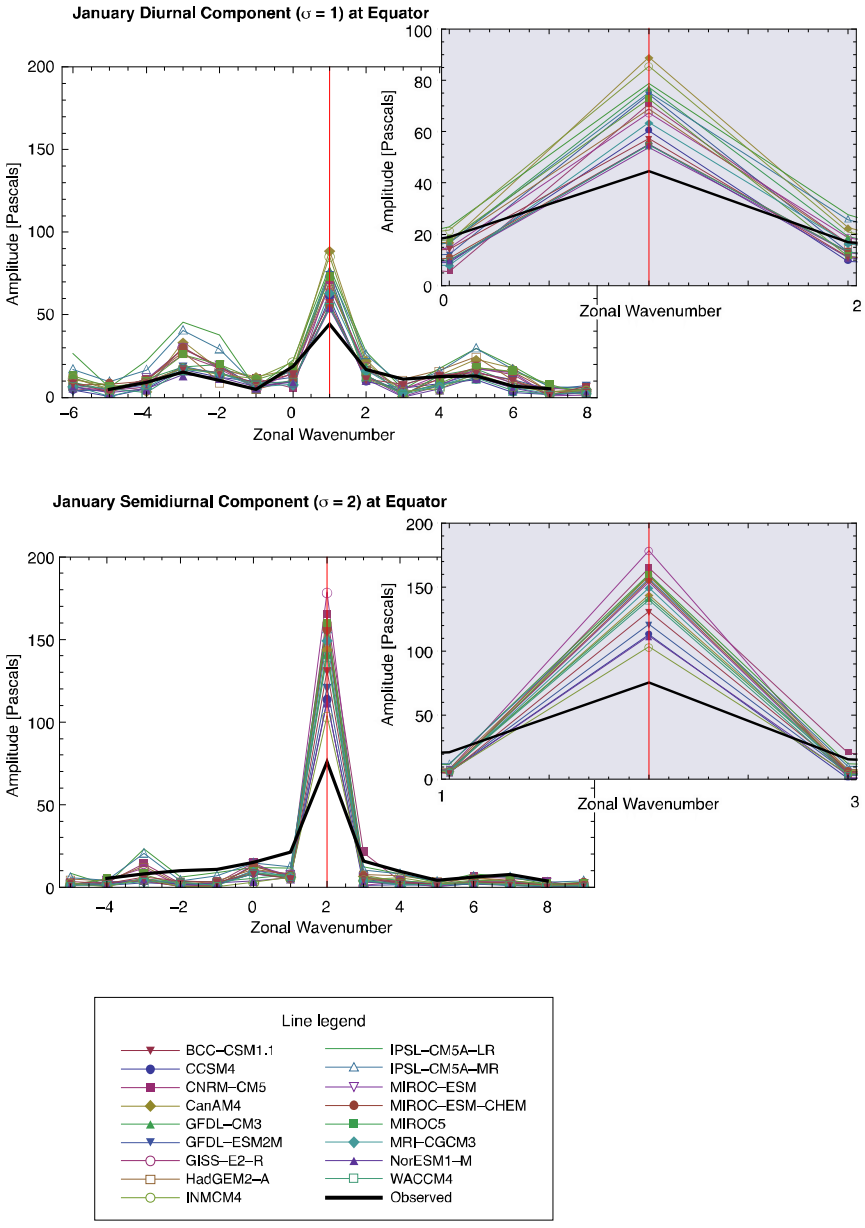


FIG. 3. Amplitude at the equator vs. zonal wavenumber for (top) diurnal and (bottom) semidiurnal harmonics of (thin colored lines) all CMIP5 / IPCC AR5 climate models in this study and (thick black line) observations for January. Closeups show details of peaks in the vicinity of migrating Fourier-component wavenumbers (red vertical lines).

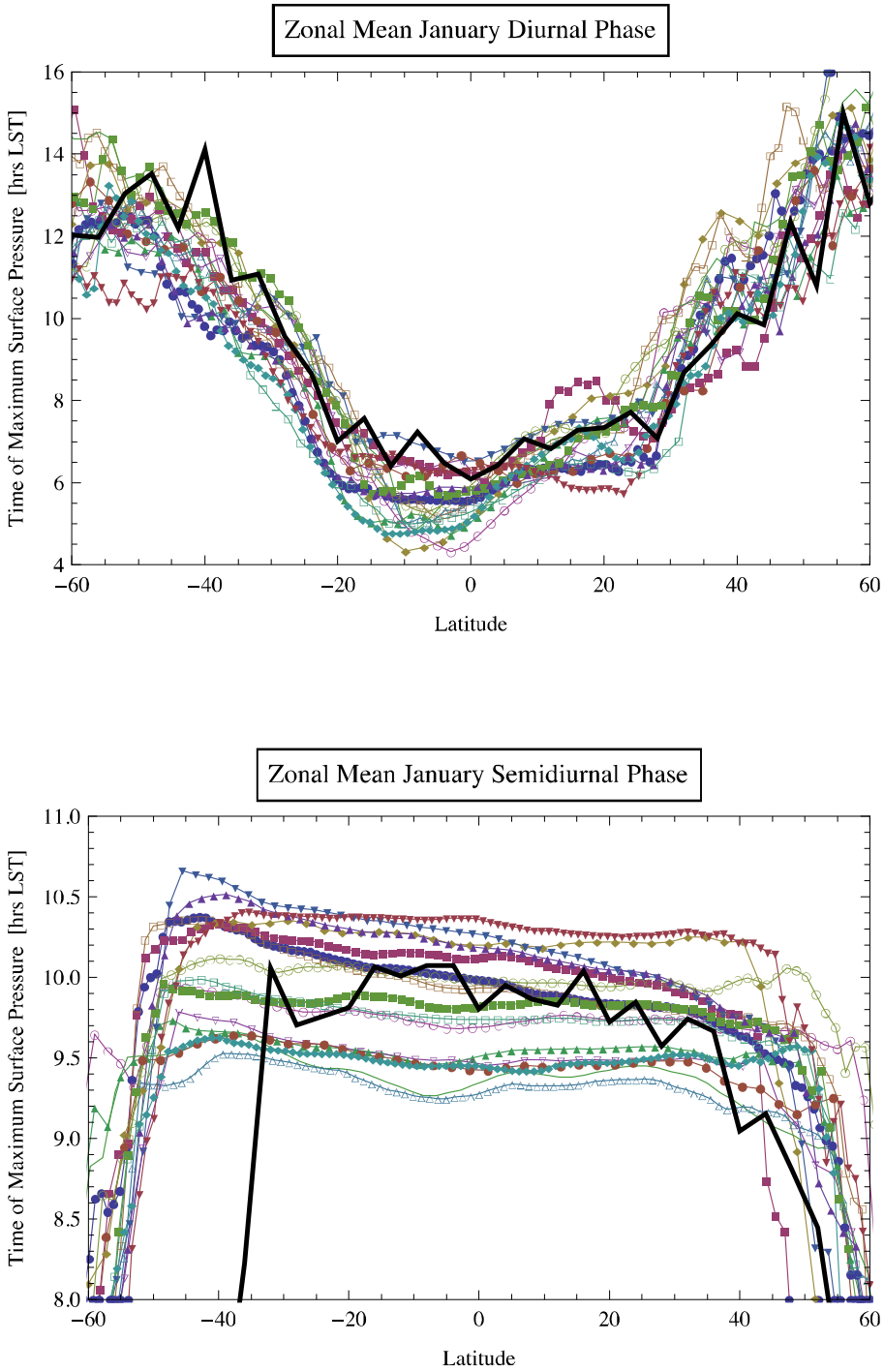


FIG. 4. January tidal phase vs. latitude for (thick black line) observations and for all CMIP5 / IPCC AR5 climate models in this study. See Fig. 3 for line legend distinguishing the different models.